Corrosion Protection of Electrogalvanized Steel by Surface Treatments containing Cerium and Niobium compounds

J.M. Ferreira Jr[1,2,], K.P. Souza[1], J.L. Rossi[1], I. Costa[1], G.F.Trindade[2], C.R. Tomachuk[3]*

[1] Instituto de Pesquisas Energéticas e Nucleares - IPEN/CNEN-SP, Av. Prof. Lineu Prestes, 2242, CEP 05508-000, São Paulo, SP, Brazil
[2] University of Surrey, Faculty of Engineering and Physical Sciences, Guildford, Surrey, GU2 7XH, United Kingdom
[3] Engineering School of Lorena of the University of São Paulo (EEL-USP), Environmental and Basic Sciences Department, Estrada Municipal do Campinho, s/n, 12602-810, Lorena, SP, Brazil
[*]E-mail: jose.ferreira@surrey.ac.uk

In this work, new surface treatments for the corrosion protection of electrogalvanized steel have been evaluated. The aim was to search for chromium free treatments to replace those based on hexavalent chromium. Surface films were obtained by immersion in solutions containing salts for increasing conductivity, coating forming salts (i.e. cerium nitrate and niobium oxalate ammonium) and an organic complexing agent (2-butyne 1,4 diol propoxylate). The morphology and composition of the surface films formed were characterized by scanning electron microscopy (SEM) and X-ray Photoelectron Spectroscopy (XPS). The corrosion resistance of the treated surfaces was evaluated by electrochemical impedance spectroscopy (EIS) and their chemical composition was characterized by XPS. It was found that it consists of an organic coating with cerium incorporated. The electrochemical results suggested surface film increased the corrosion resistance of the electrogalvanized steel and similar protection properties to that of a chromate coating were indicated.

1. INTRODUCTION

Surface treatments in solutions containing rare-earth metals have been recently studied. The metals studied are cerium, lanthanum and praseodymium; however, the most studied rare-earth metal is cerium. The coatings obtained in solutions containing cerium are more resistant than coating produced in molybdates solutions, besides presenting non-toxic properties. Consequently, production processes use rare earth salts are environmentally friendly and layers formed by deposition on different

doi:

kinds of metallic surface [1-3].

The corrosion resistance provided by the coatings obtained in solutions containing cerium ions is attributed to the formation and precipitation of oxides or hydroxides of cerium in the cathode sites of metal substrate. The production of these oxides and / or hydroxides, alternately, causes a reduction in the rate of the cathodic reaction, increasing the corrosion resistance of the material [4].

The cerium films may be generated by ion implantation process, by immersion of the substrate in solutions containing cerium salts [4,5], by incorporation of cerium salts in the zinc bath [6,7], by electrodeposition in solutions containing cerium ions [8-10], and also by the sol-gel process [11,12].

Shibli [6] developed a CeO_2 nanoparticle film wherein Ce $(NO_3)_3$.$6H_2O$ was incorporated into the zinc bath. The production process was used in preparing the hot dipping. Among the studied concentrations for the addition of $Ce(NO_3)_3$.$6H_2O$ zinc bath at 0.1% was resulted in better adhesion properties, hardness, porosity and corrosion resistance. The coating produced had a thickness of 50 μm, however the thickness of the CeO_2 film was 20 nm to 40 nm order.

There are several studies on the treatment area of the surfaces treatments and passivation of zinc alloy using solutions containing cerium salts. Recent studies show innovations as cerium nanoparticulate film application on metallic substrate [13] or adding materials such as composite silanes [14], cerium silicate or film of zirconate [15,16], all with the aim of increasing its corrosion resistance properties.

Some studies have indicated that the use of Ce ions as a modifier based on silane pre-treatment can formed a film with of self- healing property. Trabelsi et al. [14] show that the electrochemical behavior of pretreated galvanized steel with a silane coating (bis [triethoxysilylpropyl] -tetrasulfeto) doped with Ce ions, has improved anticorrosive properties compared to the undoped film, increasing its barrier properties and improving its capacitive behavior. This property was improved dependent the added dopant concentration, showed the highest performance for 10^{-3} mol/L of cerium.

Compounds of niobium, specifically ammonium niobium oxalate (ANO) have also been investigated as surface treatments for the corrosion protection of steels and electrogalvanized steels. Have been considered as a potential replacement for nickel in phosphating baths to reduce hazardous waste in the environment and increase the corrosion protection [18-20]. The results of these studies have indicated a potential ability of niobium-based coatings to protect metallic substrates against corrosion [18-21].

The aim of the present study is to develop a surface treatment for electrogalvanized steel. A mixed organic/inorganic corrosion protective coating is formed through room temperature immersion of the substrates in a bath containing a complexing agent, specifically 2 butyne-1,4 diol propoxylate together with cerium nitrate, used as coating forming salts. The corrosion resistances of the surfaces after the immersion treatments were compared to that of electrogalvanized steel with hexavalent chromium conversion coatings. The structure and composition of the coatings were investigated by scanning electron microscopy (SEM), and X-ray photoelectron spectroscopy (XPS). The corrosion resistance of the treated surfaces was evaluated by electrochemical impedance spectroscopy (EIS) using sodium chloride solution.

2. EXPERIMENTAL PROCEDURE

2.1. Electroplating

Plates (6.5 cm x 10 cm x 0.1 cm) of SAE/AISI 1010 steel were electrogalvanized in laboratory with a commercial cyanide-free alkaline electrodeposition bath (12.5 g/L Zn^{2+}, 170 g/L KOH, 50 g/L K_2CO_3, 10 mL/L additive, 10 mL/L conditioner, 1 mL/L brightening agents). The following conditions were used: temperature (22±3) ºC and cathodic current density of 2 A/dm^2 for 45 min.

Prior to zinc coating, all the steel plates were degreased in a sodium silicate-based alkaline solution, at room temperature applying a current density of 3 A/dm^2 for 3 min so as to improve the surface wettability. The plates were rinsed in deionized water, activated in ammonia difluoride 5% solution for 30 s, and rinsed again with deionized water. Immediately after the electrogalvanizing step, the samples surface was activated in 0.5% HNO_3 solution (pH 1), for 10 s, and then, rinsed with deionized water.

2.2. Samples preparation

Immediately after the electrogalvanizing step (electrogalvanized steel without conversion treatment, called Zn) the surfaces were passivated by either of the following treatments:

(i) Cr^{6+}-based conversion treatment (generally called chromate conversion coating CCC), here called Zn+Cr. The parameters used were pH 1.8, room temperature, 60 s in an industrial immersion bath with mechanical agitation of the material to be plated. This passivation bath was composed of 2 g/L sodium dichromate, sodium chloride as a conductive salt and diluted HCl solution for pH adjustment;

(ii)   Ce(III) based conversion treatment, here called Zn+Ce. The parameters used were pH 4.2, 60 s immersion time, room temperature and mechanical agitation. This passivation bath was composed of 3.4 g/L $NaNO_3$, 5.7 g/L Na_2SO_4, 12.6 g/L of 2-butyne 1,4 diol propoxylate and 17.3 g/L of $Ce(NO_3)_3.6H_2O$;

(iii)   niobium and Ce(IV)-based conversion treatment, here called Zn+Ce+Nb. This treatment consisted of immersion for 60 s in the cerium solution as described in (iii) above, rinsing, immersion for 60 s in hydrogen peroxide 1% v/v solution for 60 s, rinsing and immersion for 60 s in niobium solution. The niobium solution was composed of 3.4 g/L $NaNO_3$, 5.7 g/L Na_2SO_4, 12.6 g/L of 2-butyne 1,4 diol propoxylate and 17.3 g/L and 4.9 g/L ammonium niobium oxalate (ANO), pH 3.8.

After the surface treatments, all samples were rinsed with deionized water and dried in an oven for 20 min at 100 °C.

2.3. Surface characterization

Morphological evaluation of the surfaces after the various treatments investigated was carried out using a JEOL JSM-6330F FEG-SEM with a Si detector and 20 keV energy.

The chemical composition of the surface after treatments was evaluated by X-ray Photoelectron Spectroscopy (XPS) carried out using a Thermofisher Scientific Theta Probe. The XPS spectra acquired used X-ray source with monochromator AlKα (hν = 1486.6 eV). The analysis with X-ray spot radius of 300 μm and high-resolution spectra were acquired at 50 eV for passage of the species of interest, such as carbon and cerium. The other spectra were acquired with steps of 30 eV, the case of carbon, zinc and oxygen. The values used for adjustments of C 1s elements, O 1s, Ce 3d and Zn 2p will be shown for comparison.

The XPS analyzes were performed at three different points (spots) per sample and the spectra are representative of surface discarding local variations. Quantitative surface chemical analyses were calculated from the high-resolution core level spectra following the removal of a non-linear Shirley background.

2.4. Electrochemical behaviour

The electrochemical experimental set-up used consisted of a three-electrodes cell arrangement with an Ag/AgCl (KCl$_{sat}$) electrode and a platinum wire used as reference and counter electrodes respectively. For the working electrode (treated surfaces), an area of 1 cm^2 was exposed to the electrolyte.

All electrochemical measurements were performed at room temperature (22±3)°C in naturally aerated 0.1 mol/L NaCl solution.

The EIS analyses performed were carried out the range frequency 100 kHz to 10 mHz, with a signal amplitude perturbation of 10 mV, and a data acquisition rate of 10 points per decade. EIS data was acquired at the open circuit potential, using a BioLogic SP200 potentiostat controlled by EcLab software. Prior to EIS measure, open circuit potential (OPC) measurements were obtained to monitor potential stabilization. The potential stability was checked by measuring the corrosion potential after all electrochemical tests to confirm that the potential variation did no exceed 5 mV.

In order to evaluate reproducibility and reliability of the results, at least three tests were carried out for each condition tested.

3. RESULTS AND DISCUSSION

**Table 1.** Description of the surfaces evaluated in the present investigation.

Samples	Description
Zn	Eletrogalvanized steel sheet without passivation
Zn+Cr	Zinc coating passivated in chromating solution, pH 1,8, during 60 s, mechanical stirring.
Zn+Ce	Eletrogalvanized steel passivated in cerium solution, pH 4.2, during 60 s, mechanical stirring.
Zn+Ce+Nb	Eletrogalvanized steel passivated in cerium solution during 60 s, following by rinsing, immersion in hydrogen peroxide solution, rinsing and immersion in niobium solution, pH 3.8, for 60 s; mechanical stirring.

The identification symbol and description of investigates samples are summarized in Table 1.
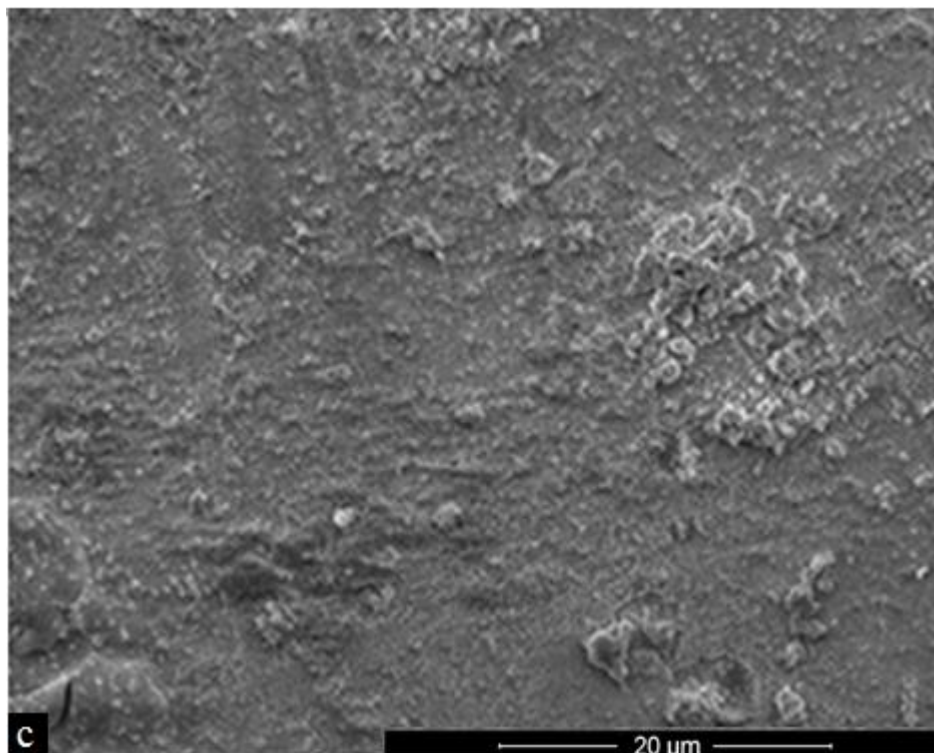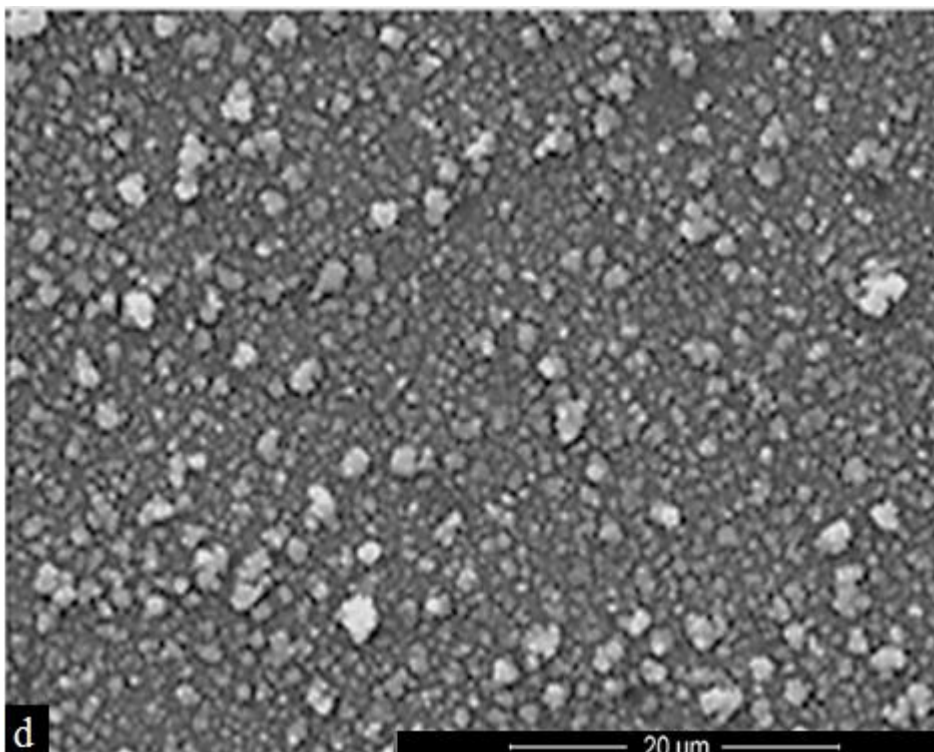
3.1. Morphology of coatings
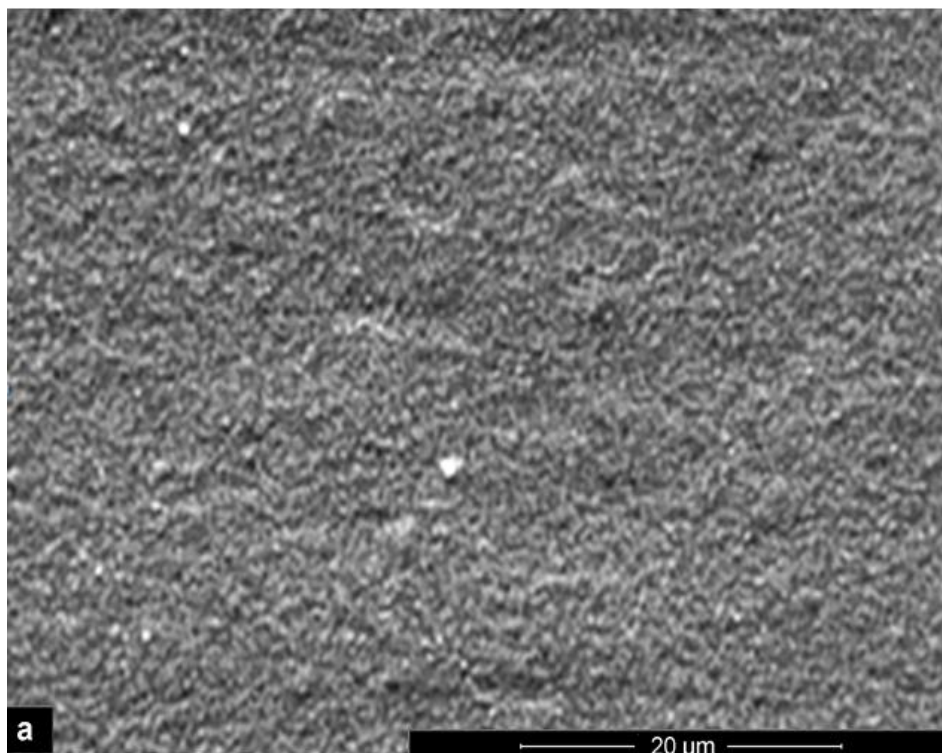
(a) Zn
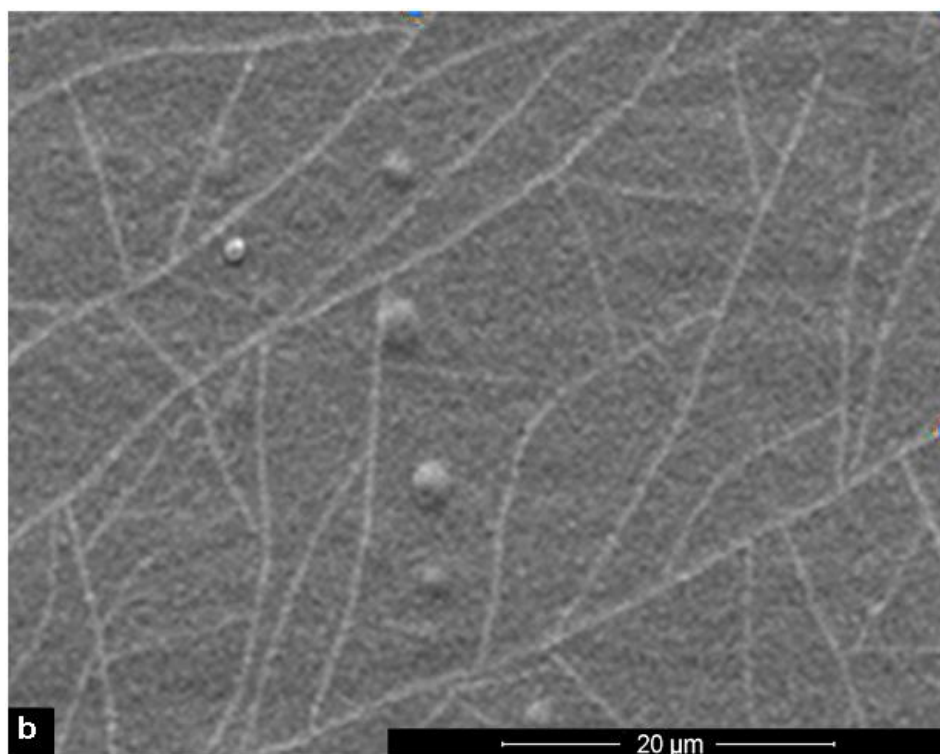
(b) Zn+Cr

(c) Zn+Ce

(d) Zn+Ce+Nb

Figure 1. SEM images of the electrogalvanized surface (a) Zn; following the chromium surface (b) Zn+Cr (pH 1.8); and respectively for surfaces prepared in solutions containing cerium Zn+Ce (pH 4.2) (c); and (d) ammonium niobium oxalate Zn+Ce+Nb (pH 3.8).

SEM images of the electrogalvanized Zn surfaces prior to and after the Zn+Cr, Zn+Ce and Zn+Ce+Nb treatments are shown in Figure 1(a-d), respectively.

The micrographs show the evolution of the electrogalvanized steel surface morphology, after the successive stages of immersion treatments. The surface of the electrodeposited zinc coating (Figure 1a) is fairly homogeneous without pores despite the presence of small while particles on the surface. Figure 1b presents a gel-like structure with micro-cracks on the surface, according to previous reports [22-24]. These micro-cracks are characteristic of chromate, being a result of a dehydration mechanism, which occurs during drying time, by volume retraction [23-25]. In Figure 1c observed irregular surface in all extension and there are areas where thicker deposits are observed. The coating formed after due immersion steps, Figure-1d, was more homogeneous and could not be removed by scraping. White particles were observed on the surface showed that these were Ce and Nb rich precipitates (omitted in this paper but confirmed by XPS).

The SEM images showed in Figure 1 shows the evolution of morphologies associated with the different treatments used.

3.2. XPS analysis
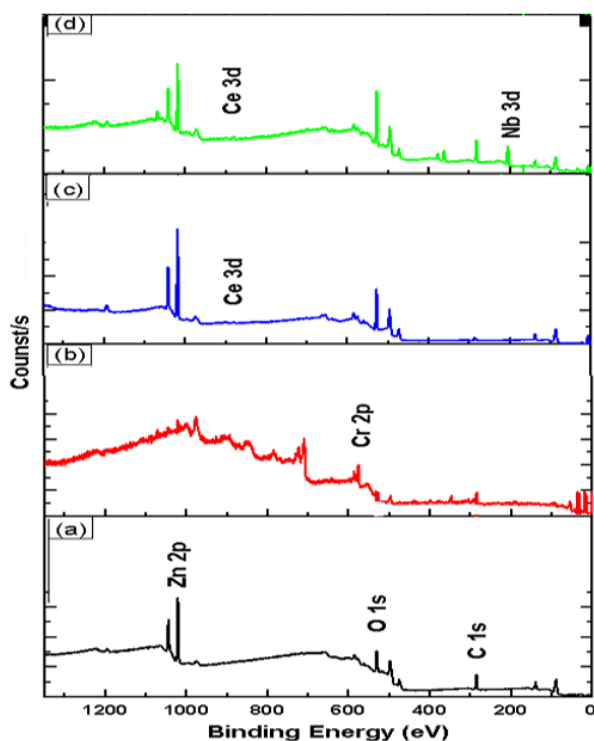
Figure 2. XPS survey spectra from zinc surface Zn (a); zinc immersed in chromium solution Zn+Cr(b), zinc immersed in solution containing cerium (c); zinc immersed in solution containing cerium and then exposed to a niobium containing solution Zn+Ce+Nb (d).

The composition and chemical state of the elements in the cerium conversion coatings were analyased by XPS. Figure 2 shows XPS Survey spectra aquerid of the: (a) Zn, (b) Zn+Cr, (c) Zn+Ce,

and (d) Zn+Ce+Nb coatings. Note that the intensities of the XPS peaks do not directly represent relative concentrations, as the elemental sensitivity factors and the analyzer transmission function must be taken into account.

The Survey spectra showed the presence of carbon and oxygen to all surfaces. The presence of carbon is reported as a contaminant in the case of surfaces formed from immersion in solutions onse organic compounds are absent. The presence of carbon in this case, for Zn and Zn+Cr coating, also occurs due to the adsorption of CO_2 from the atmosphere in the drying process.

XPS analysis showed the incorporation of Ce, Cr, and Nb in the films formed. The elemental concentrations of the fims after surface treatments are shown in Table 2 for samples treated in solutions Zn+Ce and Zn+Ce+Nb.

Table 2. XPS elemental concentrations for surfaces Zn+Cr, Zn+Ce, twoo steps Zn+Ce+Nb.

Samples	C	O	Zn	Cr	Ce	Nb
	(At.%)					
Zn+Cr	2.00	75.0	-	23	-	-
Zn+Ce	16.38	57.49	24.95	-	1.77	
Zn+Ce+Nb	38.39	42.56	12.54	-	1.82	5.68

For the C, O, Zn, Ce and N elements, high resolution XPS spectra were acquired (C 1s, O 1s, Zn $2p_{3/2}$, Ce $3d_{5/2}$ / Ce $3d_{3/2}$ and Nb $3d_{5/2}$). Figure 3 shows the C 1s XPS peak deconvolution for the Zn+Ce and Zn+Ce+Nb treated surfaces. The amount of fitting components, binding energy and FWHM used are indicated in Table 3.

Upon exposure of the samples in ambient air, several organic contaminants can adsorb on the hydroxylated oxide surface, giving rise to the contamination of carbonaceous species [26,27]. Figure 3 shows typical C1s peak fittings for the Zn+Ce and Zn+Ce+Nb treatments. It is seen that C1s peaks (Figure 2) can be decomposed into different components corresponding to C–C/C–H, C–COO$_X$, C–O, C=O and O–C=O/O–C–O– species [28].
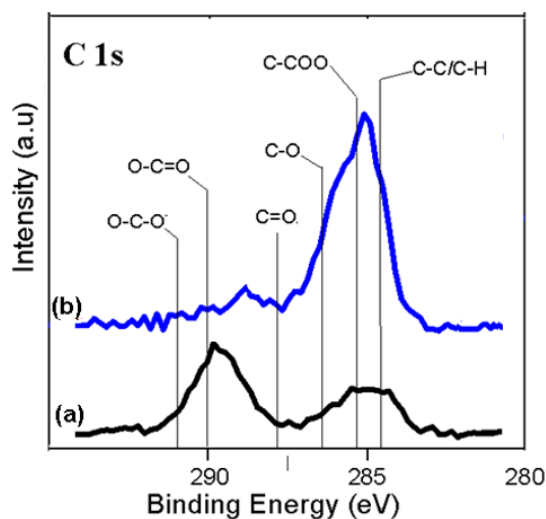
**Figure 3.** XPS peak C 1s deconvolution for the surfaces after (a) Zn+Ce, (b) Zn+Ce+Nb treatments.

Figure 4 shows XPS spectra of O 1s for the (a) Zn+Ce and (b) Zn+Ce+Nb treated samples with fitting for peaks O1s peaks corresponding to O^{2-}, OH^-, COx, and H_2O. The fitting components, binding energy and FWHM used are presented in Table 3. Three fitting Gaussians peaks marked were used to fit the experimental data of O 1s. Peak O^{2-}, positioned at the lower binding energy of 529.8 eV is assigned to the Zn–O bonding of the zinc oxide structure [29].
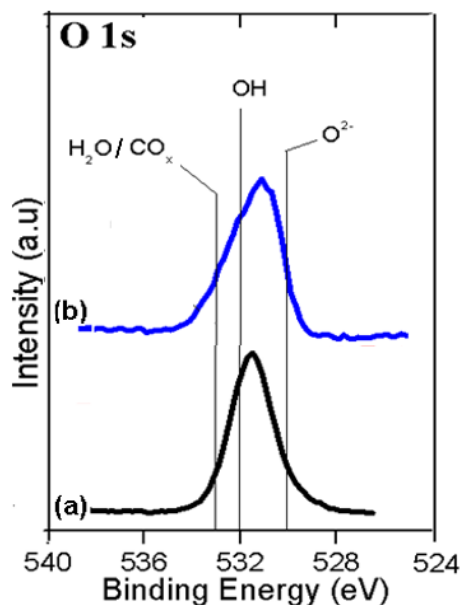
Figure 4. XPS peak C 1s deconvolution of the samples (a) Zn+Ce, (b) Zn+Ce+Nb.

Figure 5 displays XPS spectra of $Zn2p_{3/2}$ for the films obtained after the (a) Zn+Ce and (b) Zn+Ce+Nb treatments. The fitting components, binding energy and FWHM used are showed in the Table 3.
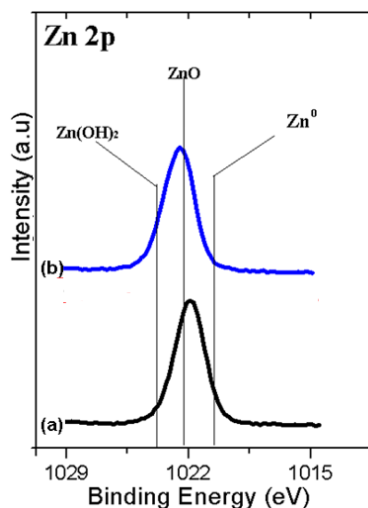
Figure 5. XPS spectrum of raw data and peak fitting position for Zn 2p3/2 for treatments: (a) Zn+Ce and (b) Zn+Ce+Nb.

Table 3 shows peak deconvolution corresponding to the C1s peak with binding energy and FWHM factors corresponding to fitting for C–C/C–H, C–COOX, C–O, C=O and O–C–O/O–C–O‾ components for the Zn+Ce and Zn+Ce+Nb treatments. It is observed that the binding energy separations were corresponding to published values [28]: (284.6 ± 1.2 eV), adventitious carbon; peak 2 (285.3 ± 1.2 eV), C double bond; peak 3 (286.4 ± 1.2 eV), carbon in carbonyl; peak 4 (287.7 ± 1.2 eV), carbon in carbonate groups and/or adsorbed CO and CO_2; and peak 5 (289.5 ± 1.2 eV).

The amount of aliphatic carbon (C-C/C-H) increased with the number of treatment steps. Although the aliphatic carbons are reported as possible contaminants, the coatings showed strong adhesion in a tape test, and the amounts of carbon did not reduce significantly after spputering for times corresponding to 180 seconds etch time. This increase is correlated to higher deposition of organic coumpoud with C-C and C-H bonds present. When analyzing the amount of carbon related to the carboxyl group it is seen that a higher carbon concentration is detected with only one stage of treatment. It is proposed that this is due to the high activity of the eletrogalvanized surface with higher number of free sites. Additional steps have resulted in the growth of the organic layer formed. It can be assumed the formation of organic layer in the with presence of carboxylic groups and the fitting for the C-COO$_X$ setting show that coating with a preparation step is more effective.

The concentration of aliphatic carbon (C-C/C-H) undergoes a large increase with the number of treatment steps and this variation is more pronounced when comparing with the results for coatings with 1 and 2 treatment steps.

This increase is corelated to higher deposition of organic coumpoud with C-C and C-H bond present. When analyzing the amount of carbon related to the carboxyl group is the opposite, with a higher concentration with only one stage of treatment. This occurs because the steel surface eletrogalvanized be more active and have a higher number of free sites, since these steps have led deposition of an organic coating already formed. It can be assumed the formation of organic coating in the with presence of carboxylic groups and the fitting for the C-COO$_X$ setting show that coating with a preparation step are most effective.

Peak deconvolution of O 1s peaks with binding energy and FWHM factors corresponding to fitting for O^{2-}, OH‾, CO$_x$, and H_2O components of the coatings Zn+Ce and Zn+Ce+Nb are showed in Table 3.

The peak deconvolution of Zn2p$_{3/2}$ peaks corresponding to Zn^0, ZnO and Zn(OH)$_2$ components of the coatings Zn+Ce and Zn+Ce+Nb are showed in the Table 3.

The Zn 2p$_{3/2}$ peaks from coating Zn+Ce present the peak centered around 1022 eV (ZnO/Zn(OH)$_2$) and the most marked difference is seen in the Zn+Ce+Nb peak. For Zn+Ce+Nb coating the peak is shifted to higher binding energy, and it shows the presence of a larger amount of ZnO compared to the other two samples.

The presence of the peak in low binding energy (1020.6 eV) is associated with Zn^0 and can occur due to analysis of the sample exposed areas, discontinuity of sight coating formed in Figure-1b, exposed zinc substrate.

Table 3. XPS results for Zn+Ce, and Zn+Ce+Nb samples, signal for C 1s, O 1s, Zn 2p fitting species, binding energy values, FWHM and the atomic concentrations

Surfaces	Signal	Fitting	BE (eV)	F.W.H.(eV)	at%
Zn+Ce	C 1s	C–C/C–H	284.7	0.78	38.37
		C–COOX	285.3	0.78	1.6
		C-O	286.3	0.77	2.14
		C=O	287.7	0.77	0.83
		O-C-O/O-C=O	290.7	0.78	57.05
	O 1s	O^{2-}	529.8	1.45	15.20
		OH^-	531.3	1.89	64.35
		C-O	532.8	1.36	20.45
	Zn2p	Zn^0	1020.6	1.36	25.51
		ZnO	1022.3	1.31	28.96
		$Zn(OH)_2$	1023.8	1.90	45.53
Zn+Ce+Nb	C 1s	C–C/C–H	284.7	0.78	84.38
		C–COOX	285.3	0.89	0.42
		C-O	286.3	0.88	8.03
		C=O	287.7	0.87	2.09
		O-C-O/O-C=O	290.7	0.81	0.41
	O 1s	O^{2-}	529.8	1.45	0.45
		OH^-	531.3	1.89	62.47
		C-O	532.8	1.36	0.41
	Zn2p	Zn^0	1020.6	1.36	11.62
		ZnO	1022.3	1.32	83.64
		$Zn(OH)_2$	1023.8	1.92	4.84
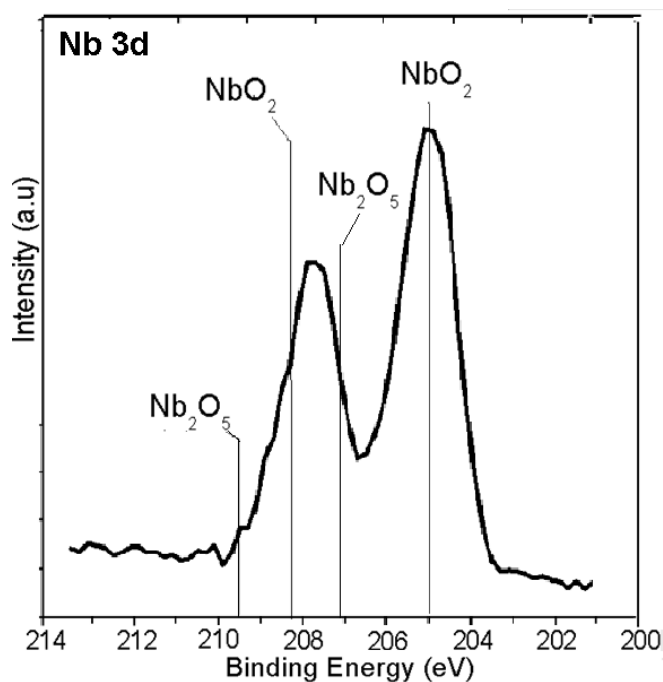
Figure 6. XPS spectrum of raw data and peak fitting position for Nb $3d_{5/2}$ for sample Zn+Ce+Nb.

The use of ammonium niobium oxalate for niobium deposition is a distinctive contribution of this work. The results showed that Nb was found in the coating predominantly as NbO_2 (Figure 6). Table 4 shows the binding energies used to fitting the satelites $1Nb^{4+}$, $2Nb^{5+}$, $3Nb^{4+}$ $4Nb^{5+}$, and evaluate the niobium concentration.

The Nb $3d_{5/2}$ spectrum was aquired only for the Zn+Ce+Nb treatment and it shows that it is typical of niobium oxides in two states (NbO_2 and Nb_2O_5). The amount of NbO_2 prevails allowing further oxidation during exposure to oxidizing environments and providing longer protection as the evolution to a more stable product, Nb_2O_5, occurs.

Table 4. Binding energies and FWHM factors used for fitting niobium oxide forms in the **Zn+Ce+Nb** coating.

| Samples	$_1Nb^{4+}$	$_2Nb^{5+}v$	$_3Nb^{4+}$	$_4Nb^{5+}$	NbO_2	Nb_2O_5
BE(eV	205.1	207.3	208.3	209.5	$_1Nb^{4+}+_3Nb^{4+}$	$_2Nb^5+_4Nb^5$
At.% **Zn+Ce+Nb**	55.4	20.2	22.1	2.3	77.5	22.5

XPS results supported the development of an organic coating (carboxylated groups linked to the metal substrate) with metallic oxides, such as ZnO, $Zn(OH)_2$, CeO_2, Ce_2O_3, Nb_2O_5 and NbO_2, incorporated in their structure. The source of these carboxylic groups (seen in XPS results, Table 3) is 2-butyne 1,4 diol propoxylate in the treatment solution. This decomposes in the oxidizing environment used (NO_3^-/SO_4^{2-}) forming alcohols and subsequently oxidize to form aldehydes and then carboxylic acids.

3.3. Electrochemical behavior

(a)

(b)
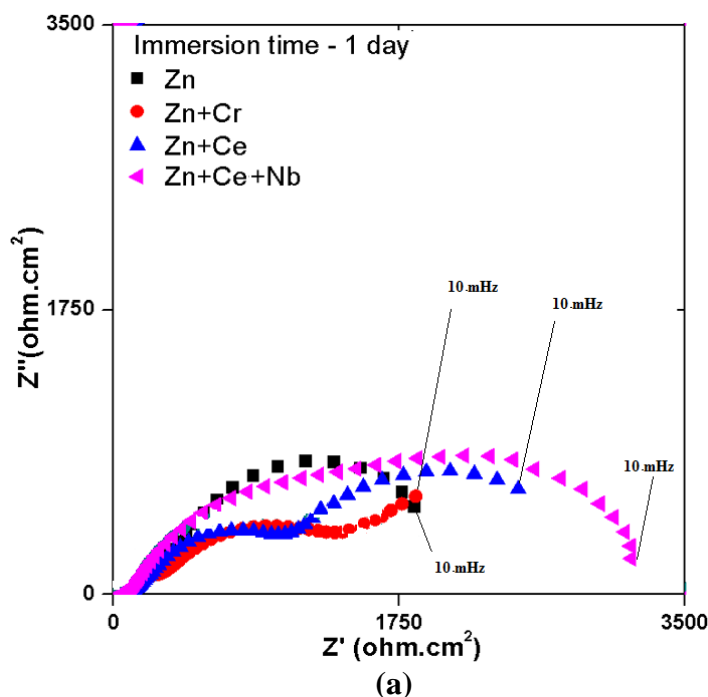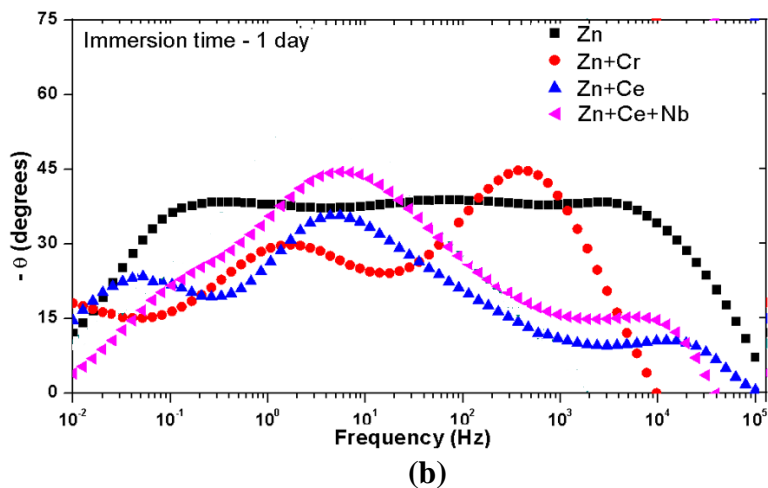
Figure 7. EIS results: (a) Nyquist diagram and (b) Bode phase angle for samples with surfaces corresponding to Zn, Zn+Cr, Zn+Ce and Zn+Ce+Nb treatments at 1 day of immersion in 0.1 mol/L NaCl solution.
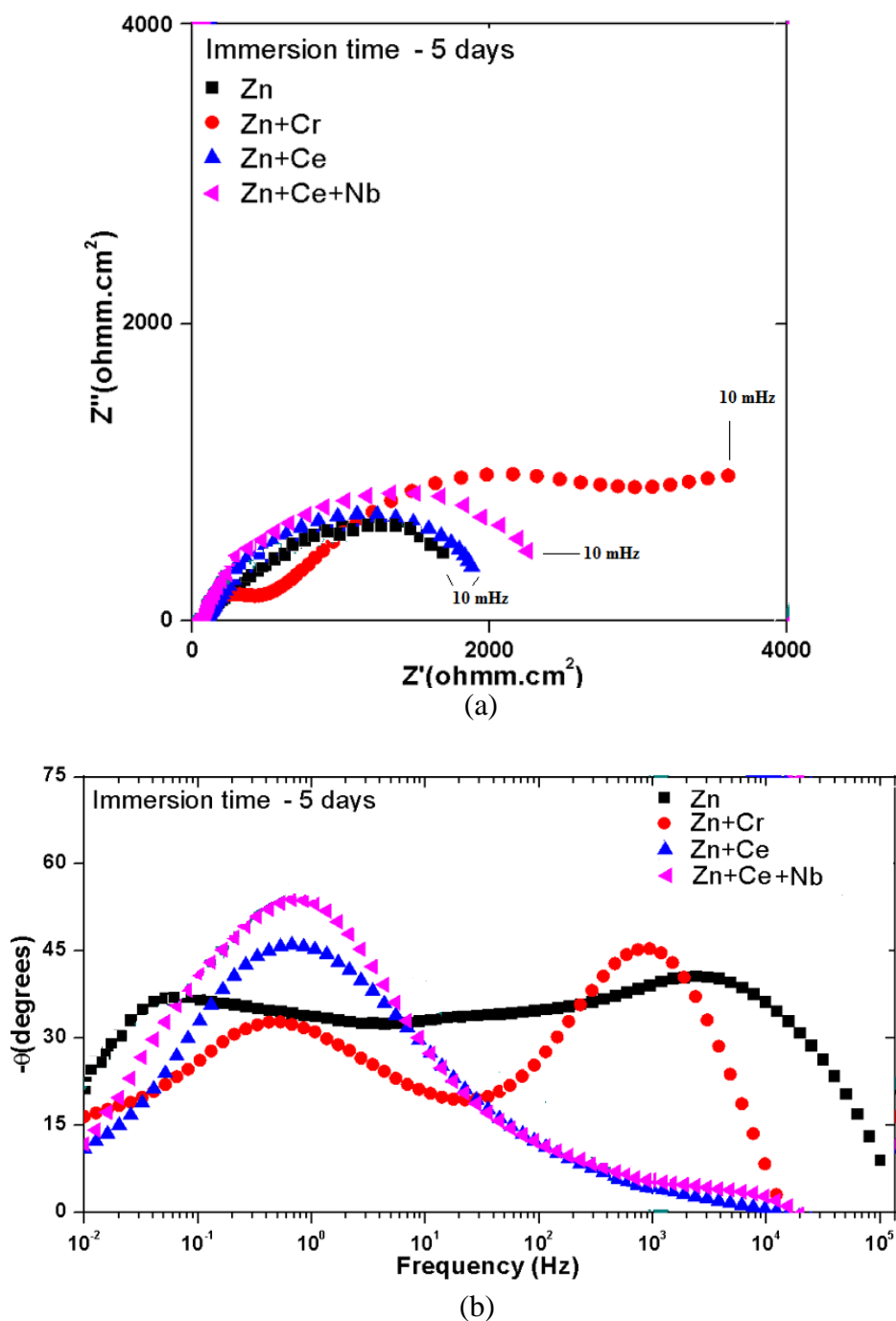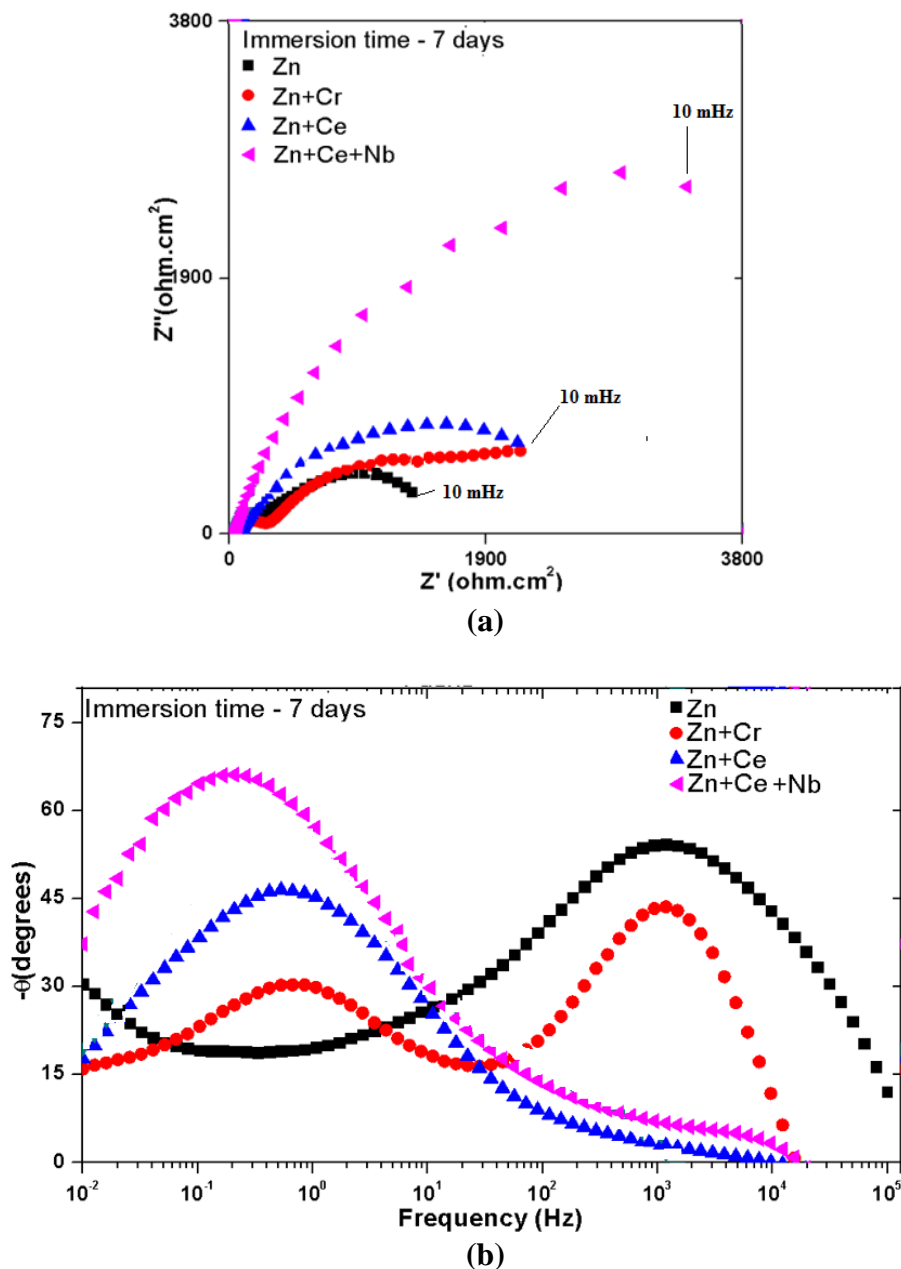

(a)

(b)
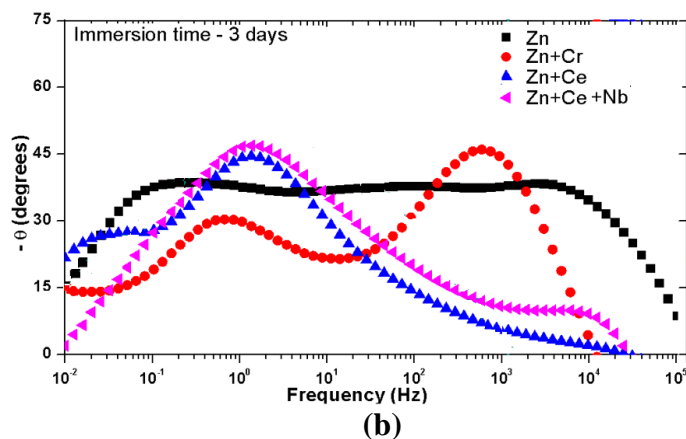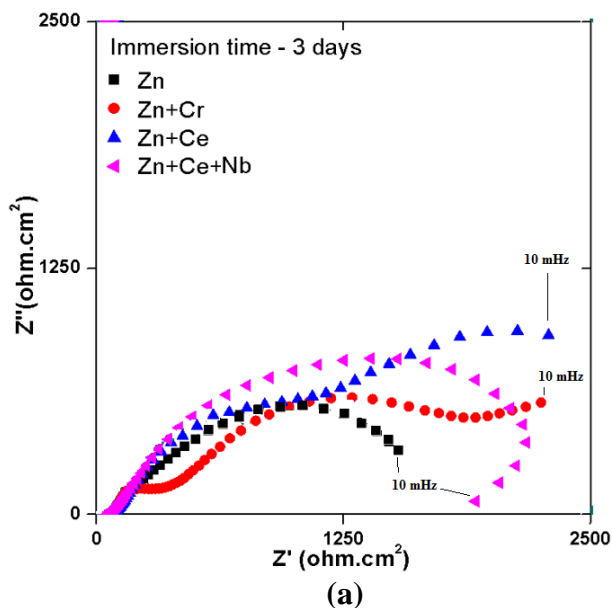
Figure 8. EIS results: (a) Nyquist diagram and (b) Bode phase angle for samples with surfaces corresponding to Zn, Zn+Cr, Zn+Ce and Zn+Ce+Nb treatments at 3 days of immersion in 0.1 mol/L NaCl solution.

The corrosion resistance of the treated surfaces was investigated by electrochemical tests, specifically electrochemical impedance spectroscopy (EIS) as a function of exposure time. Eletrogalvanized steel samples without surface treatment (Zn) and with chromating treatment (Zn+Cr) were also used as references, for comparison reasons. The EIS results corresponding to 1, 3, 5 and 7 days of exposure to 0.1 mol/L NaCl solution are shown in Figures 7 to 10, respectively, as Nyquist diagrams.

Figure 9. EIS results: (a) Nyquist diagram and (b) Bode phase angle for samples with surfaces corresponding to Zn, Zn+Cr, Zn+Ce and Zn+Ce+Nb treatments at 5 days of immersion in 0.1 mol/L NaCl solution.

(a)

(b)

Figure 10. EIS results: (a) Nyquist diagram and (b) Bode phase angle for samples with surfaces corresponding to Zn, Zn+Cr, Zn+Ce and Zn+Ce+Nb treatments at 7 days of immersion in 0.1 mol/L NaCl solution.

The impedances associated the treateds surfaces exposed to two steps treatment were inferior to that of the untreated samples (Zn) from 1 until 5 days of immersion (Fig. 9) and were very similar at 7 day (Fig. 10). It was indicated that the film formed provides corrosion protection to the substrate and also acted as anchoring sites for zinc corrosion products. The main zinc corrosion product ($Zn(OH)_2$) is known as a corrosion inhibitor and the organic film seems to hold it at the surface prolongind the corrosion protection of the substrate.

The impedances associated with the surfaces exposed to the Zn+Ce+Nb treatment show a large decrease between 1 (Fig. 7) and 3 days of immersion (Fig. 8) likely due to the interaction of the

corrosive medium with the substrate. This however was followed by a continuous increase from 3 days until 7 days of immersion (Fig. 10) supporting the hypothesis of further corrosion protection by the retention of the inhibitive zinc corrosion products at the surface. The formation of CeO_2 and Nb_2O_5 by the three steps treatment has also improved the protective properties of the film formed.

The time constant at high frequencies is referenced as an effect on the zinc oxide coating formed during expoure to the electrolyte[26]. A comparison of the phase angles values for untreated samples (Zn) allows the observation of a time constant at this frequency range with phase angles greater than those presented by the samples with treatments Zn+Ce and Zn+Ce+Nb.

The EIS results show a displacement of the time constant at low frequencies associated with the various treatments tested to lower frequencies showing a slowing down of the kinetics of the charge transfer processes and the charging of the double layer associated to this time constant. This must be caused by the blockage of defects/porosities of the surface film by corrosion products hindering the access of the corrosive species to the substrate.
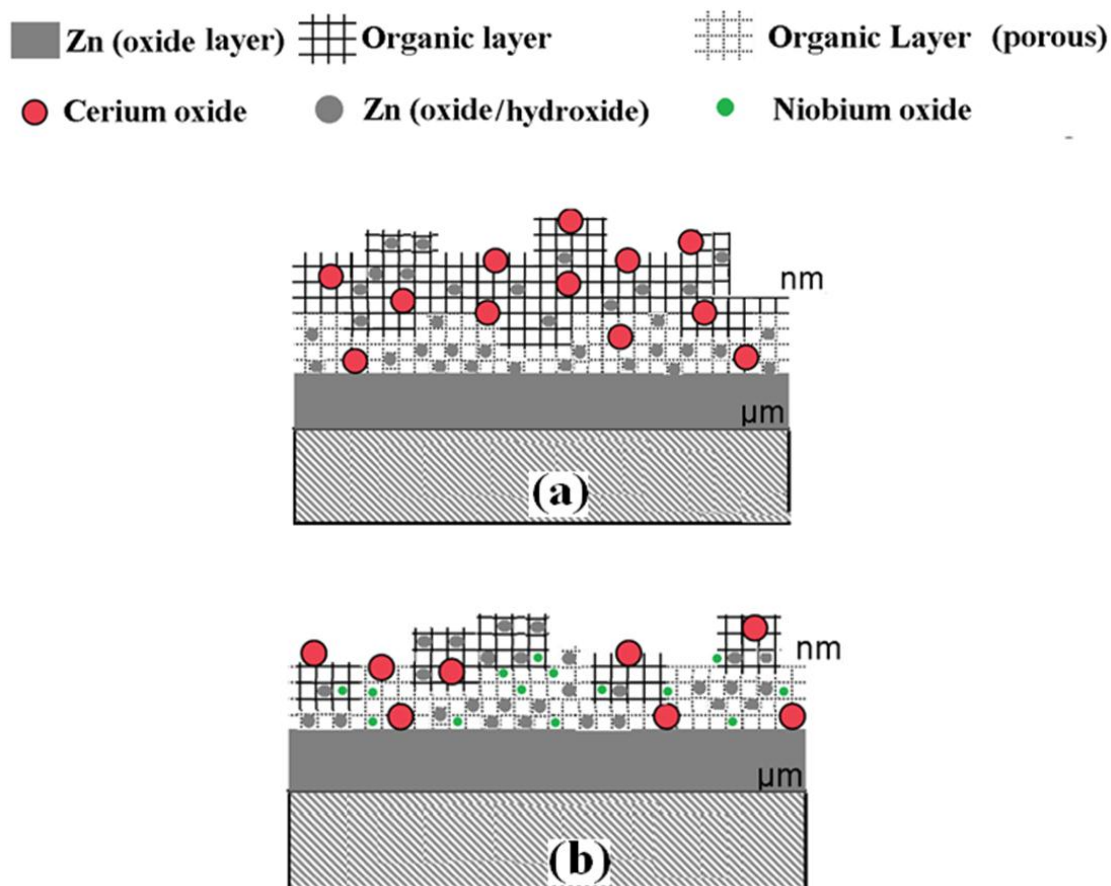
Figure 11. Coating models proposed for samples with treatments (a) Zn+Ce and (b) Zn+Ce+Nb. A synergistic effect seemingly occurs between cerium oxide, zinc oxide and niobium oxide incorporated in the surface film. The presence of an organic film acting as anchoring sites for inhibiting corrosion products leads to a delayed failure of the surface.

The organometallic film formed with cerium and niobium oxide incorporated resulting from the Zn+Ce+Nb treatment seems to be permeable to corrosive species leading to zinc corrosion products at the surface. Zinc corrosion products were seemingly anchored by the organometallic coating prolonging the corrosion protection of the substrate for prolonged periods of time.

A corrosion mechanism was proposed in a previous study for surfaces prepared in similar solutions with different immersion times (10 minutes per step) [5] and this iw shown in Figure 11. A model is proposed for the surface film formed during one step treatment (Zn+Ce), Figure 11a, and another for the surface film formed by a two steps treatment (Zn+Ce +Nb), Figure 11b, respectively.

4. CONCLUSIONS

The surface treatments tested in this study resulted in the formation of surface films that increased the corrosion resistance of electrogalvanized steel. This was attributed to the formation of a surface film composed of organic and inorganic compounds (cerium oxides or niobium oxides). The penetration of the electrolyte into this film resulted in the formation of corrosion products which were incorportated into it to which leading to prolonged corrosion protection of the substrate indicated by the evolution of electrochemical results with time of test.

References

1. A.R. Phan, F.J. Gammel, T. Hack and H. Haefke, *Mater. Corr.*, 56 (2)(2005) 77-82.
2. S-H. Zhang, G. Kong, J-T. Lu, C-S. Che and L-Y. Liu, *Surf. Coat. Technol.*, 259 (2014) 654-659.
3. L.E.M. Palomino, I.V. Aoki and H.G. De Melo, *Electrochem. Acta*, 51 (2006) 5943-5953.
4. C. Motte, N. Maury, M.G. Olivier and J.P. Petitjean, J.F. Willem, *Surf. Coat. Techn.*, 200 (2005) 2366-2375.
5. J.M. Ferreira-Jr, J.L. Rossi, M.A. Baker, S.J. Hinder and I. Costa, *Int. J. Electrochem. Sci.* 9 (2014) 1827-1839.
6. S.M.A. Shibli and F. Chacko, *Surf. Coat. Technol.*, 202 (2008) 4971-4975.
7. M.A. Arenas and J.J. Damborenea, *Surf. Coat. Technol.*, 187 (2004) 320-325.
8. J. Creus, F. Brezault, C. Rebere and M. Gadouleau, *Surf. Coat. Technol.*, 200 (2006) 4636-4645.
9. Y. Hamlaoui, C. Remazeilles, M. Bordes, L. Tifouti and F. Pedraza, *Corros. Sci.*, 52 (2010) 1020-1025.
10. X. Huang, N. Li, H.H. Wang, H. Dun, S. Sun and J. Zheng, *Thin Solid Films*, 516 (2008) 1037-1043.
11. Y. Castro, B. Ferrari, R. Moreno and A. Durán, *Surf. Coat. Technol.,* 182, (2004) 199-203.
12. G.R. Salazar-Banda, S.R. Moraes, A.J. Motheo and S.A.S. Machado, *J. Sol-Gel Sci. Technol.*, 52 (2009) 415-423.

13. M.F. Montemor, R. Pinto and M.G.S. Ferreira, *Electrochim. Acta*. 54 (2009) 5179-5189.
14. W. Trabelsi, P. Cecilio, M.G.S. Ferreira and M.F. Montemor, *Prog. Org. Coat.* 54 (2005) 276-284.
15. K. Aramaki, *Corros. Sci.* 44(6) (2002) 1375-1389.
16. R.Z. Zand, V. Flexer, M. De Keersmaecker, K. Verbeken and A. Adriaerns, *Int. J. Electrochem. Sci.*, 10 (2015) 997-1014
17. L.M. Palomino, P.H. Suegama, I.V. Aoki, M.F. Montemor and H.G. De Melo, *Corros. Sci.*, 51 (2009) 1238–1250.
18. E. P. Banczek, P. R. P. Rodrigues and I. Costa, *Surf. Coat. Technol.*, 202 (10) (2008) 2008-2014.
19. E. P. Banczek, M. Terada, P. R. P. Rodrigues and I. Costa, *Surf. Coat. Technol.,* 205 (7) (2010) 2503-2510.
20. E.P. Banczek, P.R.P. Rodrigues and I. Costa. *J. Mater. Eng. Perform.* 22 (11) (2013) 3572-3583.
21. A. Verma and P.K.Singh, *Indian J. Chem.,* 52A (2013) 593-598.
22. T. Bellezze, G. Roventi and R. Fratesi, *Surf. Coat. Technol.,* 155 (2-3) (2002) 221-230.
23. M.A. Crespo, E. Bustamante, A.M. Huerta, F.J. Gómez, S.E. Rodil and A. Vela, *Metallurgical Mat. Trans.,* 40A (2009) 1631-1644.
24. N.M. Martyak, *Surf. Coat. Technol.*, 88 (1996) 139-146.
25. C. Wang, G. Chen, G. Wen and G. Wu, *Surf. Interface Anal.,* 41 (9) (2009) 705-709.
26. M. Bethencourt, F.J. Botana, J.J. Calvino, M. Marcos, M.A. and Rodriguez-Chacon, *Corr. Sci* ., 40 (1998*)* 1803-1819.
27. K.M. Pertays, G.E. Thompson and M.R. and Alexander, *Surf. Interface Anal.,* 36 (2004) 1361-1366.
28. P. Taheri, J. Wielant, T. Hauffman, J.R. Flores, F. Hannour, J.H.W. De Wit and H. Terryn, *Electrochim. Acta,* 56 (1994) 1904-1911.
29. C.V. D'Alkaine and M.N. Boucherit, *J. Electrochem. Soc.,* 144 (10) (1997) 3331-3336.